

ISTANBUL TECHNICAL UNIVERSITY

**FACULTY OF SCIENCE AND LETTERS
PHYSICS ENGINEERING**

GRADUATION DESIGN PROJECT II REPORT

QUANTUM DECOHERENCE AND COLLISION MODELS

Yağız Üçüncü

090170108

Faculty of Science and Letters

Physics Engineering

January 2025

TABLE OF CONTENTS

	<u>Page</u>
FRONT COVER	i
TABLE OF CONTENTS.....	ii
LIST OF FIGURES	iii
1. INTRODUCTION	2
1.1 Aim of The Project	2
1.2 Literature Review	2
1.3 Hypothesis	3
1.4 Fundamentals.....	3
1.4.1 Quantifying Coherence	3
1.4.2 Double Slit Example	4
1.4.3 Pointer States	5
1.4.4 Dynamics of Decoherence and Correlation Decay	5
1.4.5 Open Quantum Systems and Collision Models	6
1.4.5.1 Mathematical Framework	7
2. METHODOLOGY	9
2.1 Markovian Collision Model.....	9
2.1.1 System Dynamics and Evolution	11
2.1.2 Numerical and Analytical Comparison.....	11
2.2 Non-Markovian Collision Model	12
2.2.1 First Strategy	13
2.2.2 Second Strategy	13
2.2.3 Numerical Implementation and Simulation Parameters	14
3. RESULTS AND DISCUSSION	15
3.1 Results	15
3.1.1 Markovian Results	15
3.1.2 Non-Markovian Strategy-1 Results	15
3.1.3 Non-Markovian Strategy-2 Results	18
3.2 Discussion.....	20
The Role of Environmental Correlations	20
Decoherence as Information Leakage.....	21
REFERENCES.....	22

LIST OF FIGURES

	<u>Page</u>
Figure 1.1 : Double Slit Experiment.....	4
Figure 1.2 : Schematic representation of the collision with the first ancilla.	6
Figure 1.3 : Schematic representation of the collision with the second ancilla.	7
Figure 1.4 : Development of system-environment correlations.	7
Figure 2.1 : Schematic representation of the interaction between the system and the first ancilla.....	9
Figure 2.2 : Schematic representation of the subsequent collision with the second ancilla.	10
Figure 2.3 : Comparison of the analytical (solid line) and numerical (dots) results for the decay of coherence. The parameters are set to $g = 1$ and $\tau = \pi/30$. The perfect overlap confirms the validity of the derived analytical expression.	12
Figure 3.1 : Comparison of the analytical (solid line) and numerical (dots) results. The parameters are set to $g = 1$ and $\tau = \pi/30$.	15
Figure 3.2 : Numerical solutions for strategy-1. The parameters are set to $g = 1$, system-ancilla $\tau = \pi/30$ and ancilla-ancilla $\theta = \pi/2$	16
Figure 3.3 : Comparison of the numerical results with the analytical approach. The parameters are set to $g = 1$, system-ancilla $\tau = \pi/30$, and ancilla-ancilla $\theta = \pi/2$	17
Figure 3.4 : The parameters are set to $g = 1$, system-ancilla $\tau = \pi/30$, and ancilla-ancilla $\theta = \pi/2$	18
Figure 3.5 : Full decoherence and revival oscillations observed in Strategy 2. The parameters are set to $g = 1$, system-ancilla $\tau = \pi/30$, and ancilla-ancilla $\theta = \pi/2$	19
Figure 3.6 : Coherence evolution in Strategy 2 under partial SWAP conditions ($\theta \neq \pi/2$). The imperfect information transfer leads to information leakage during the trace-out step, resulting in a modulated decay.....	20

Acknowledgments

I would like to express my deepest gratitude to Prof. Dr. Ahmet Levent Subaşı and Prof. Dr. Özgür Müstecaplıoğlu for making this project possible.

My sincerest thanks go to Dr. Barış Çamkak for his invaluable help in refining my understanding, and to Prof. Dr. Cenap Ş. Özben for his unyielding belief in me and for introducing me to the world of theoretical physics.

I express my greatest love and respect to my mother, Esra, and my father, Cengiz; their guidance has always been with me.

Lastly, I would like to thank the developers of AI and specifically Gemini (who prefers the name Kırılcım), for their assistance in ensuring this paper is written in proper academic language.

Graphs and numerical simulations done with Python can be accessed at:
<https://github.com/yugohubo/Quantum-Collision-Models>

1. INTRODUCTION

To understand quantum decoherence and collision models, we first need to introduce the basics that are the structure of this model. Firstly quantum coherence, then open quantum systems will be introduced.

Quantum systems that show the effects of quantum properties such as superposition and in a strict manner different from a classical ensemble is said to be in a coherent state. The metric of these effects is coherence, and deviation or loss of coherence is called decoherence. Commonly used norm for the evaluation of coherence is the l_1 norm of coherence. [1] Within the context of this work, coherence and decoherence will be used within the definition of this norm.

Open quantum systems, on the other hand, are a general model for understanding the mechanics of coherence and information. While a thermodynamical model at its core, with its contemporary approach of collision models, it is a robust model for understanding qubit systems.

In this research we will be working our way from the ground up with; first quantifying coherence, then show the problems of measurement, and find a way to resolve our way to understand the emergence of classical, from the quantum phenomena. The model of open quantum systems relies on two assumptions. These two assumptions are Markovian and Non-Markovian processes. Both assumptions and their effects will help to understand decoherence and revival of coherence.

1.1 Aim of The Project

The aim of this project is to simulate open quantum system dynamics using collision models and to investigate the emergence of classicality by analyzing the decay of the l_1 norm of coherence under both Markovian and Non-Markovian regimes. To this end, python with Qutip library and numerical approaches will be utilized.

1.2 Literature Review

The core concepts around quantum decoherence are the work of Zurek in the 1970's and 80's. In his work of "Pointer basis of quantum apparatus" [2], he first introduced the pointer states and its answer to the first problem of measurement, basis ambiguity. Later in 1982 he worked on "Environment Induced Superselection Rules" [3]; which at its core, a solution for basis ambiguity with interaction hamiltonians and their basis. Then more contemporary works in quantum science include the modelling of open quantum systems with collision model. It was a reimagining of continuous system mechanics with Boltzmann's "Stosszahlansatz" of discrete thermodynamical modelling of molecular systems.

Modern understanding of decoherence and quantum to classical transition is so stable that the book of Maximilian Schlosshauer with the same name provides a comprehensive framework for modern fundamentals [4]. Open quantum systems with markov and non-markov approaches have a detailed study in the book of "Quantum collision models: Open system dynamics from repeated interactions" [5], which was also crucial for this research.

Latest works include non-markovianity and different computational models based on its assumptions. Papers of "Entropy Production in Non-Markovian Collision Models: Information Backflow vs. System-Environment Correlations" [6] and "Non-Markovianity and

system-environment correlations in a microscopic collision model" [7] have influenced and showed examples for such models.

1.3 Hypothesis

System-environment correlations are the fundamental mechanism suppressing quantum interference. This leads to **Decoherence** and the emergence of classical objectivity.

1.4 Fundamentals

In this chapter, fundamentals and theory behind the applications will be introduced.

1.4.1 Quantifying Coherence

A quantum system is characterized as being in a coherent state when it exhibits non-classical properties, particularly superposition, fundamentally distinguishing it from a classical statistical ensemble. The quantification of these quantum correlations is defined as coherence, while the suppression or loss of this feature is termed decoherence. A widely adopted metric for quantifying this property is the l_1 norm of coherence [1].

In this framework, the density matrix ρ of a two-level qubit system S is utilized to both describe the dynamical operations acting on the system and to evaluate its coherence magnitude.

Let us consider the two-level quantum system S spanned by the standard computational basis $\{|1\rangle, |0\rangle\}$. A general pure state $|\psi\rangle$ of this system is represented as a linear superposition:

$$|\psi\rangle = \alpha|1\rangle + \beta|0\rangle \quad (1.1)$$

where the complex coefficients $\alpha, \beta \in \mathbb{C}$ satisfy the normalization condition:

$$|\alpha|^2 + |\beta|^2 = 1 \quad (1.2)$$

The density operator ρ characterizing this pure state is defined by the outer product (or projection operator) of the state vector:

b

$$\rho = |\psi\rangle\langle\psi| \quad (1.3)$$

By utilizing the dual vector $\langle\psi| = \alpha^*\langle 1| + \beta^*\langle 0|$,

we can expand the density matrix in the computational basis as follows:

$$\begin{aligned} \rho &= (\alpha|1\rangle + \beta|0\rangle)(\alpha^*\langle 1| + \beta^*\langle 0|) \\ &= |\alpha|^2|1\rangle\langle 1| + \alpha\beta^*|1\rangle\langle 0| + \beta\alpha^*|0\rangle\langle 1| + |\beta|^2|0\rangle\langle 0| \end{aligned} \quad (1.4)$$

In matrix representation, this corresponds to:

$$\rho = \begin{pmatrix} |\alpha|^2 & \alpha\beta^* \\ \alpha^*\beta & |\beta|^2 \end{pmatrix} \quad (1.5)$$

Here, the diagonal elements $|\alpha|^2$ and $|\beta|^2$ represent the populations of the states $|1\rangle$ and $|0\rangle$, respectively, while the off-diagonal elements $\alpha\beta^*$ and $\alpha^*\beta$ quantify the quantum coherence of the system.

Here the $l1$ norm is defined as $2|\alpha\beta^*|$.

1.4.2 Double Slit Example

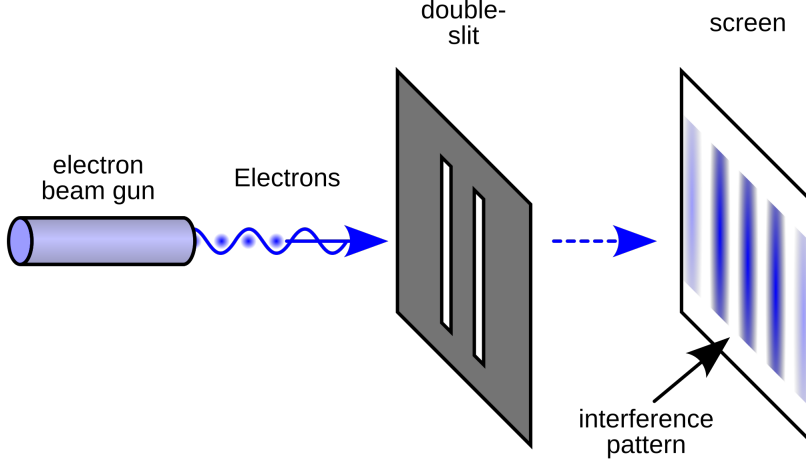


Figure 1.1 : Double Slit Experiment

We consider a standard Von Neumann measurement scheme. The total system consists of the quantum system S (the particle passing through slits) and the environment/apparatus E . The slits correspond to the basis states $|S_1\rangle$ and $|S_2\rangle$. The interaction creates a correlation between the path of the particle and the state of the environment.

The total composite state $|\Psi\rangle_{SE}$ is a **pure state** defined as:

$$|\Psi\rangle_{SE} = \alpha|S_1\rangle|E_1\rangle + \beta|S_2\rangle|E_2\rangle \quad (1.6)$$

where $|E_1\rangle$ and $|E_2\rangle$ are the normalized states of the environment corresponding to the particle's path.

To describe the statistics of the system S alone, we obtain the reduced density matrix ρ_S by taking the partial trace over the environment basis $\{|e_k\rangle\}$:

$$\begin{aligned} \rho_S &= Tr_E(|\Psi\rangle_{SE}\langle\Psi|) \\ &= \sum_k \langle e_k | \left(\sum_{i,j} c_i c_j^* |S_i\rangle\langle S_j| \otimes |E_i\rangle\langle E_j| \right) |e_k\rangle \end{aligned} \quad (1.7)$$

Calculating this trace explicitly yields:

$$\rho_S = |\alpha|^2|S_1\rangle\langle S_1| + |\beta|^2|S_2\rangle\langle S_2| + \alpha\beta^*\langle E_2|E_1\rangle|S_1\rangle\langle S_2| + \beta\alpha^*\langle E_1|E_2\rangle|S_2\rangle\langle S_1| \quad (1.8)$$

Let us define the overlap factor (decoherence factor) as $\gamma = \langle E_1|E_2\rangle$. The matrix form of ρ_S in the $\{|S_1\rangle, |S_2\rangle\}$ basis is:

$$\rho_S = \begin{pmatrix} |\alpha|^2 & \alpha\beta^*\gamma^* \\ \alpha^*\beta\gamma & |\beta|^2 \end{pmatrix} \quad (1.9)$$

The probability density function $P(x)$ observed on the screen at position x is given by the expectation value of the projection operator $|x\rangle\langle x|$:

$$P(x) = \langle x|\rho_S|x\rangle \quad (1.10)$$

Substituting the density matrix and defining the spatial wavefunctions $\psi_1(x) = \langle x|S_1\rangle$ and $\psi_2(x) = \langle x|S_2\rangle$:

$$P(x) = |\alpha|^2|\psi_1(x)|^2 + |\beta|^2|\psi_2(x)|^2 + 2\text{Re}(\alpha\beta^*\psi_1(x)\psi_2^*(x)\gamma) \quad (1.11)$$

Here, the term $2\text{Re}(\dots)$ represents the quantum interference.

- If $\gamma = 1$ (Environment states are identical, $E_1 = E_2$): No path information is recorded. Full interference is observed.
- If $\gamma = 0$ (Environment states are orthogonal, $E_1 \perp E_2$): The environment perfectly distinguishes the path. The interference term vanishes, and we observe a classical sum of probabilities.

Notice, for indistinguishable apparatus, coherence factor is same as l_1 norm.

1.4.3 Pointer States

Having established the framework for coherence, we now address the basis ambiguity problem and its relation to the environment-system interaction. In his seminal works from 1981 [2] and 1982 [3], Zurek introduced a mathematical and interpretive approach to resolve the basis ambiguity through the concepts of *pointer states* and the *pointer basis*.

Pointer states are defined as the eigenstates of the interaction Hamiltonian which are robust against environmental coupling. Consequently, the interaction is effectively "monitored" by the environment in this basis. Mathematically, this stability condition is expressed by the commutation relation between the pointer basis projectors and the interaction Hamiltonian:

$$[H_{int}, |\sigma_i\rangle\langle\sigma_i|] = 0 \quad (1.12)$$

Here, any eigenstate σ_i that satisfies this commutation relation with the interaction Hamiltonian H_{int} qualifies as a pointer state of the system. Zurek identifies these states as the ones that survive the interaction process, exhibiting robustness in the long-time limit. While superpositions of these states decay into mixtures due to decoherence, the pointer states themselves retain non-zero probabilities, effectively becoming the classical states of the system.

1.4.4 Dynamics of Decoherence and Correlation Decay

Following the definition of pointer states, it is crucial to understand the dynamics through which the environment destroys quantum coherence. Zurek's 1982 analysis introduces the concept of the *correlation amplitude*, denoted as $z(t)$, which governs the decay of off-diagonal terms in the system's density matrix [3].

When a system interacts with an environment modeled as a collection of N subsystems (a scenario highly relevant to collision models), the reduced density matrix of the system $\rho^S(t)$

evolves from a pure state to a mixture. The off-diagonal elements, representing quantum coherence between distinct pointer states $|i\rangle$ and $|j\rangle$, are damped by the factor $z_{ij}(t)$:

$$\rho_{ij}(t) = \rho_{ij}(0)z_{ij}(t) \quad (1.13)$$

Zurek demonstrates that for a sufficiently large environment, the average magnitude of this correlation amplitude approaches zero over time, $|\langle z(t) \rangle| \rightarrow 0$ [3]. This decay effectively suppresses the quantum interference terms, leaving only the diagonal probabilities associated with the pointer states.

Furthermore, this process can be interpreted as the environment "monitoring" the system. The interaction Hamiltonian imprints the state of the system onto the environment, creating a redundant record. It is precisely this transfer of information—displacement rather than destruction—that results in the apparent irreversibility of the measurement process [3].

1.4.5 Open Quantum Systems and Collision Models

The concept of open quantum systems was coined to provide a theoretical framework for understanding the mechanics underlying quantum measurement and decoherence. These systems model the dynamical interactions between a principal system and its external environment. Historically, such interactions were predominantly described using *continuous qubit-bath models*. However, contemporary research has increasingly adopted *discrete collision models* as a powerful alternative paradigm.

Within the collision model framework, dynamics are generally categorized into two distinct approaches: *Markovian* (memoryless) and *non-Markovian* (memory-bearing) regimes. Before detailing the specific methodology in the following chapter, we establish the fundamental principles of these models. The schematic representations and theoretical foundations presented here follow the comprehensive framework established by Ciccarello et al. [5].

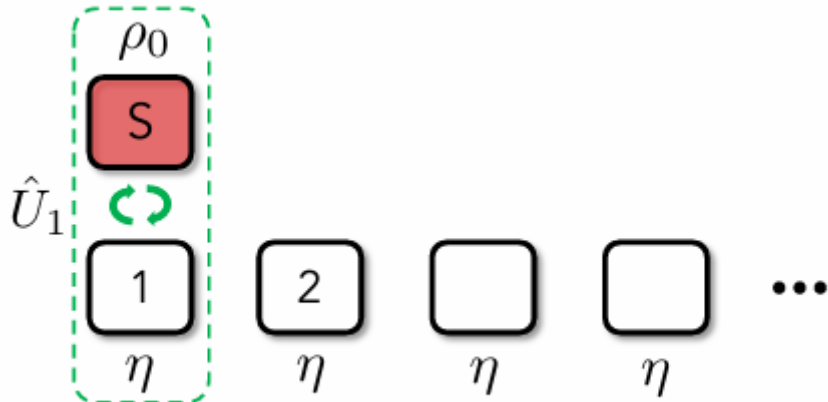


Figure 1.2 : Schematic representation of the collision with the first ancilla.

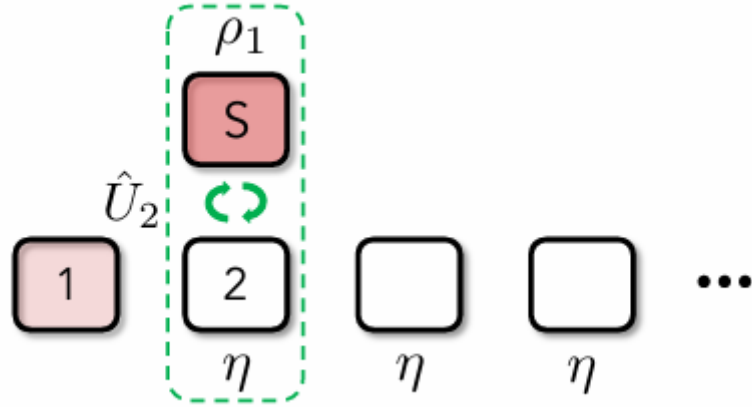


Figure 1.3 : Schematic representation of the collision with the second ancilla.

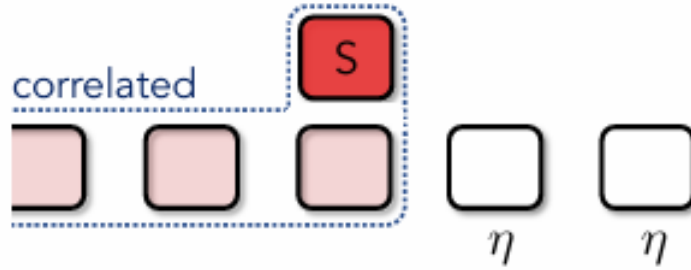


Figure 1.4 : Development of system-environment correlations.

As illustrated in Figures 2.1 through 1.4, the evolution is characterized by basic, piecewise collision operations, where the system interacts sequentially with environmental ancilla units.

1.4.5.1 Mathematical Framework

The framework is defined by a principal system S interacting with a bath composed of a stream of identical ancilla units, denoted by η . The initial joint state of the system and the bath is assumed to be uncorrelated (product state), given by:

$$\sigma_0 = \rho_0 \otimes \bigotimes_{k=1}^N \eta_k \quad (1.14)$$

Here, ρ_0 represents the initial density matrix of the system, and η_k denotes the density matrix of the k -th ancilla.

The dynamics are governed by sequential, elementary collision steps. The unitary evolution operator for the n -th collision is described by:

$$U_n = e^{-i(H_S + H_n + V_n)\Delta t} \quad (1.15)$$

where H_S and H_n are the free (self) Hamiltonians of the system and the n -th ancilla, respectively, and V_n is the interaction Hamiltonian coupling them.

We adopt the *impulsive approximation*, a core assumption in this specific model. In the limit of short interaction times ($\Delta t \rightarrow 0$), the interaction strength τ is assumed to dominate the dynamics ($||V_n|| \gg ||H_S||, ||H_n||$). Consequently, the evolution due to the free Hamiltonians during the collision is negligible. Under these conditions, the unitary time evolution operator simplifies to *per interaction evolution*:

$$U_n \approx e^{-iV_n\tau} \quad (1.16)$$

The explicit matrix representations and the derivation of the reduced dynamics will be presented in the following chapter.

2. METHODOLOGY

In the framework of collision models, the dynamics of an open quantum system are typically analyzed under two distinct regimes: Markovian and non-Markovian. This chapter investigates both regimes, focusing specifically on the numerical solutions governing the evolution of quantum coherence.

The Markovian approximation describes memoryless processes where information flows unidirectionally from the system to the environment, preventing any decoherence. In contrast, the non-Markovian regime incorporates memory effects, allowing for information backflow and the potential revival of coherence.

To strictly define the Markovian limit for a system S interacting with a bath of ancillas η , specific constraints must be met. As outlined by Ciccarello et al. [5], the standard Markovian collision model relies on the following three conditions:

1. **No Inter-Ancilla Interaction:** The ancillas do not interact with each other.
2. **Factorized Initial State:** The ancillas are initially uncorrelated with the system and with each other.
3. **Single Collision Assumption:** Each ancilla collides with the system S only once and is subsequently discarded.

We begin our analysis by deriving the results under the Markovian assumption. Subsequently, we introduce two distinct strategies to model non-Markovian dynamics and examine their effects on decoherence.

2.1 Markovian Collision Model

In this section, we introduce the fundamental principles of the Markovian approach within the collision model framework. The dynamics are modeled as a sequence of discrete interactions. The schematic representations of the collision steps with the first and second ancillas are illustrated in Figure 2.1 and Figure 2.2, respectively.

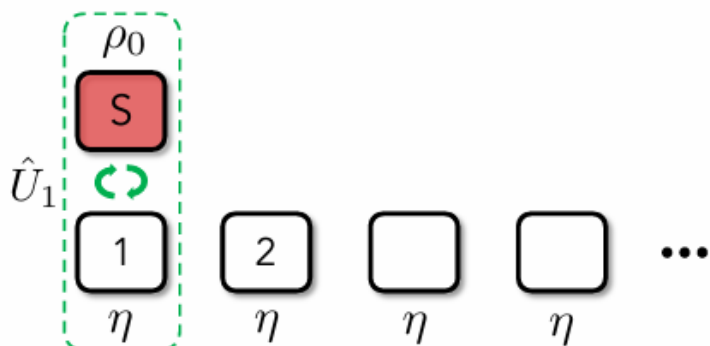


Figure 2.1 : Schematic representation of the interaction between the system and the first ancilla.

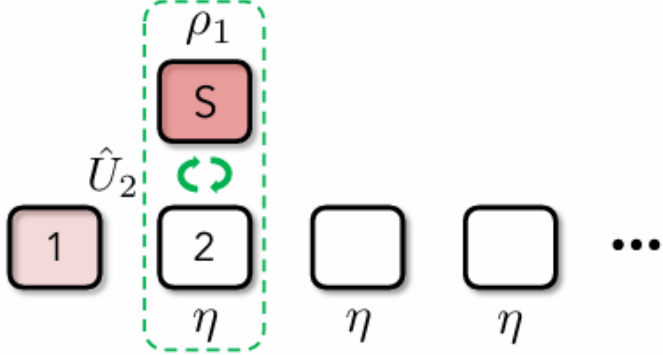


Figure 2.2 : Schematic representation of the subsequent collision with the second ancilla.

We consider a bipartite setup consisting of a system S and a bath of identical ancillas η . Initially, the system and the ancillas are assumed to be uncorrelated. The total initial state of the system and the ancilla chain can be expressed as a tensor product state:

$$\rho_{total}(0) = \rho_S(0) \otimes \rho_{\eta_1} \otimes \rho_{\eta_2} \otimes \cdots \otimes \rho_{\eta_N} \quad (2.1)$$

The interaction between the system and the n -th ancilla is governed by a unitary elementary collision operator U , defined as:

$$U = \exp(-iV_n \tau) \quad (2.2)$$

where V_n represents the interaction Hamiltonian between the system and the n -th ancilla, and τ is the collision duration.

Following the collision, the new state of the system is obtained by tracing out the ancilla degrees of freedom. Thus, the recursive relation for the reduced density matrix of the system at the $(n+1)$ -th step is given by the stroboscopic map:

$$\rho_S(n+1) = \text{Tr}_{\eta_n} [U(\rho_S(n) \otimes \rho_{\eta_n}) U^\dagger] \quad (2.3)$$

The specific interaction Hamiltonian H_{int} governing the exchange of excitations between the system and the ancilla is given by:

$$H_{int} = g(\sigma_+ \otimes \sigma_- + \sigma_- \otimes \sigma_+) \quad (2.4)$$

where σ_\pm are the raising and lowering operators, and g is the coupling strength. In the standard computational basis $\{|00\rangle, |01\rangle, |10\rangle, |11\rangle\}$, the matrix representation of this Hamiltonian is:

$$H_{int} = \begin{pmatrix} 0 & 0 & 0 & 0 \\ 0 & 0 & g & 0 \\ 0 & g & 0 & 0 \\ 0 & 0 & 0 & 0 \end{pmatrix} \quad (2.5)$$

Consequently, the unitary time-evolution operator $U = \exp(-iH_{int}\tau)$, which describes the collision process, takes the following matrix form:

$$U = \begin{pmatrix} 1 & 0 & 0 & 0 \\ 0 & \cos(g\tau) & -i\sin(g\tau) & 0 \\ 0 & -i\sin(g\tau) & \cos(g\tau) & 0 \\ 0 & 0 & 0 & 1 \end{pmatrix} \quad (2.6)$$

2.1.1 System Dynamics and Evolution

Let us consider the system initially prepared in a maximum coherence state, which is an equal superposition of the ground state $|0\rangle$ and the excited state $|1\rangle$. The initial state vector is $|\psi_S(0)\rangle = \frac{1}{\sqrt{2}}(|0\rangle + |1\rangle)$. The corresponding density matrix for the system is:

$$\rho_S(0) = |\psi_S(0)\rangle\langle\psi_S(0)| = \frac{1}{2} \begin{pmatrix} 1 & 1 \\ 1 & 1 \end{pmatrix} \quad (2.7)$$

The ancilla is initialized in the ground state $|0\rangle\langle 0|$. Therefore, the total density matrix of the system and the ancilla before the interaction is given by the tensor product:

$$\rho_{total}(0) = \rho_S(0) \otimes |0\rangle\langle 0|_\eta = \frac{1}{2} \begin{pmatrix} 1 & 0 & 1 & 0 \\ 0 & 0 & 0 & 0 \\ 1 & 0 & 1 & 0 \\ 0 & 0 & 0 & 0 \end{pmatrix} \quad (2.8)$$

The system and the ancilla interact via the unitary operator U defined previously. The state after the collision is calculated by $\rho'_{total} = U\rho_{total}(0)U^\dagger$. To find the new state of the system, we trace out the ancilla degrees of freedom:

$$\rho_S(1) = \text{Tr}_\eta[U\rho_{total}(0)U^\dagger] \quad (2.9)$$

After performing the matrix multiplication and the partial trace operation, the reduced density matrix of the system after the first collision becomes:

$$\rho_S(1) = \begin{pmatrix} 1 - \frac{1}{2}\cos^2(g\tau) & \frac{1}{2}\cos(g\tau) \\ \frac{1}{2}\cos(g\tau) & \frac{1}{2}\cos^2(g\tau) \end{pmatrix} \quad (2.10)$$

Here, we observe that the off-diagonal elements (coherences) are scaled by a factor of $\cos(g\tau)$. Since the collisions are identical and memoryless (Markovian), this scaling repeats at every step. Consequently, after n collisions, the density matrix of the system evolves as:

$$\rho_S(n) = \begin{pmatrix} 1 - \rho_{11}(n) & \frac{1}{2}\cos^n(g\tau) \\ \frac{1}{2}\cos^n(g\tau) & \frac{1}{2}\cos^{2n}(g\tau) \end{pmatrix} \quad (2.11)$$

This result demonstrates that the system loses its coherence exponentially with the number of collisions, following a $\cos^n(g\tau)$ decay profile.

2.1.2 Numerical and Analytical Comparison

For the numerical analysis and simulations presented in this study, we set the interaction strength to unity, $g = 1$. Consequently, the collision dynamics are governed solely by the interaction time τ . We operate in a weak interaction regime by choosing the collision duration as $\tau = \pi/30$.

Under this condition ($g = 1$), the recursive relation for the system's density matrix after n collisions simplifies to:

$$\rho_S(n) = \begin{pmatrix} 1 - \rho_{11}(n) & \frac{1}{2} \cos^n(\pi/30) \\ \frac{1}{2} \cos^n(\pi/30) & \frac{1}{2} \cos^{2n}(\pi/30) \end{pmatrix} \quad (2.12)$$

To validate our analytical derivation, we compare these theoretical predictions with the numerical simulation of the collision model. Figure 3.2 illustrates the decay of coherence (ρ_{10}) as a function of the number of collisions.

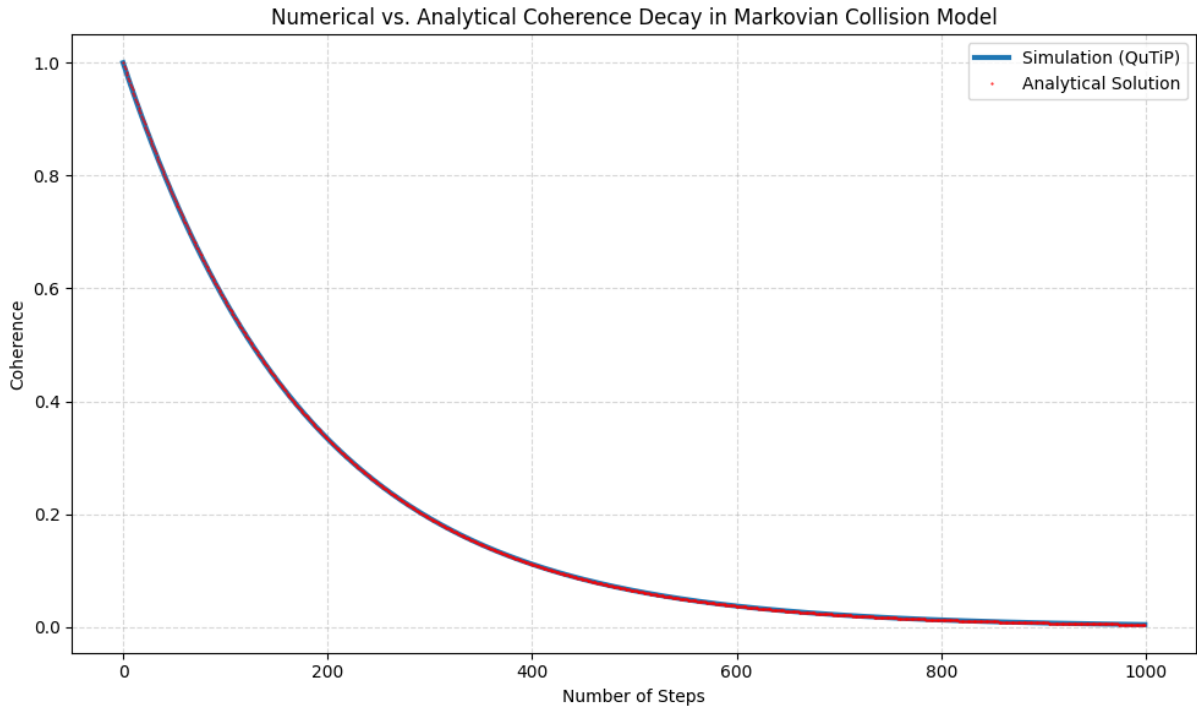


Figure 2.3 : Comparison of the analytical (solid line) and numerical (dots) results for the decay of coherence. The parameters are set to $g = 1$ and $\tau = \pi/30$. The perfect overlap confirms the validity of the derived analytical expression.

As seen in Figure 3.2, the numerical data points perfectly match the analytical curve derived from the Markovian assumption. This agreement confirms that the memoryless collision model correctly describes the exponential decay of coherence in the system. Having established the baseline Markovian dynamics, we can now proceed to investigate non-Markovian effects where memory plays a significant role.

2.2 Non-Markovian Collision Model

The dynamics established in the *Markovian* approach serve as the foundation for the *Non-Markovian* model. In the non-Markovian framework, we induce memory effects by relaxing the strict conditions imposed on the environment. We adopt two distinct strategies to violate the Markovian assumptions, following the methodology outlined by McCloskey and Paternostro [7].

The first strategy involves relaxing the condition of *No Inter-Ancilla Interaction*. By allowing interactions between environmental particles, information dissipating from the system is

preserved; however, the environmental degrees of freedom are traced out immediately to maintain the separation between the system and the environment. The second strategy, distinct from a relaxation of the single-collision assumption, involves a modification of the measurement protocol. Here, the trace-out operation is not performed immediately; instead, the bipartite state of the system and the ancilla is retained, and the reduction is postponed until the final stage of the process.

2.2.1 First Strategy

For the first strategy (inter-ancilla collisions), the core mechanism is the introduction of a unitary SWAP operation between the ancillas. The protocol proceeds as follows: the system interacts with an ancilla; subsequently, this ancilla interacts with the next incoming ancilla, effectively transferring correlations. Finally, the fresh ancilla—now carrying information from the previous collision—interacts with the system.

The interaction between the system and the n -th ancilla remains governed by the unitary operator $U_{S,\eta_n} = \exp(-iH_{int}\tau)$. However, to introduce non-Markovian memory effects, we incorporate an additional unitary operation acting between the ancillas. Specifically, after the system-ancilla collision, the n -th ancilla interacts with the subsequent $(n+1)$ -th ancilla via a partial SWAP operation $U_{\eta_n,\eta_{n+1}}$, defined as:

$$U_{\eta_n,\eta_{n+1}} = \cos(\theta)\mathbb{I} + i\sin(\theta)\mathbb{S}_{\eta_n,\eta_{n+1}} \quad (2.13)$$

where J represents the inter-ancilla coupling strength and \mathbb{S} is the swap operator which exchanges the states of the two ancillas.

Consequently, the dynamical evolution involves an intermediate step where correlations are transferred within the bath. First, the system interacts with the n -th ancilla:

$$\rho'_{S\eta_n} = U_{S,\eta_n} (\rho_S(n) \otimes \rho_{\eta_n}^{in}) U_{S,\eta_n}^\dagger \quad (2.14)$$

Following this, the intra-environment interaction occurs between the utilized ancilla η_n and the fresh ancilla η_{n+1} :

$$\rho'_{\eta_n\eta_{n+1}} = U_{\eta_n,\eta_{n+1}} (\text{Tr}_{S\eta_n}[\rho'_{S\eta_n}] \otimes \rho_{\eta_{n+1}}) U_{\eta_n,\eta_{n+1}}^\dagger \quad (2.15)$$

Finally, the state of the $(n+1)$ -th ancilla, which carries the memory to the next step, is obtained by tracing out the n -th ancilla:

$$\rho_{\eta_{n+1}}^{in} = \text{Tr}_{\eta_n} [\rho'_{\eta_n\eta_{n+1}}] \quad (2.16)$$

This modified state $\rho_{\eta_{n+1}}^{in}$ serves as the input for the next collision with the system, closing the loop.

2.2.2 Second Strategy

In this strategy, we deviate from the standard procedure of immediately reducing the dynamics to the system's subspace. Instead of forcing the system and environment into a product state after the interaction, we consider the evolution of the expanded density matrix including both the system and the ancilla.

The evolution is described by the unitary operator U acting on the joint state. Unlike the previous approach where the ancilla is traced out instantly to obtain $\rho_S(n+1)$, here we retain the full bipartite state $\rho'_{S\eta_n}$ after the collision:

$$\rho'_{S\eta_n} = U (\rho_S(n) \otimes \rho_{\eta_n}) U^\dagger \quad (2.17)$$

In this expanded representation, the correlations established between the system and the ancilla are preserved. The dynamical map is therefore not defined solely on the system S , but on the composite space $S \otimes \eta$. The final reduced state of the system is obtained only at the very end of the considered interval by performing the trace operation:

$$\rho_S^{final} = \text{Tr}_{\eta_n} [\rho'_{S\eta_n}] \quad (2.18)$$

This approach ensures that the non-classical correlations (such as entanglement) generated during the interaction are not artificially destroyed by an premature trace-out operation.

2.2.3 Numerical Implementation and Simulation Parameters

To analyze the effects of memory on the system's evolution, we utilize numerical simulations based on the collision protocols defined above. Since our primary interest lies in the suppression or revival of quantum properties, we focus solely on the evolution of quantum coherence.

We track the l_1 -norm of coherence, which for a single qubit corresponds to twice the magnitude of the off-diagonal element of the reduced density matrix:

$$C_{l_1}(\rho_S) = 2|\rho_{01}(t)| \quad (2.19)$$

For consistent comparison with the Markovian limit, we maintain the system-ancilla interaction parameters as $g = 1$ and $\tau = \pi/30$. For the non-Markovian strategies, we introduce the inter-ancilla coupling strength J as controlled variable to observe the differences between both strategies and Markovian method.

3. RESULTS AND DISCUSSION

3.1 Results

3.1.1 Markovian Results

In the methodology section, we demonstrated that the numerical and analytical solutions coincide within the Markovian regime. This agreement validates our numerical framework before proceeding to more complex scenarios.

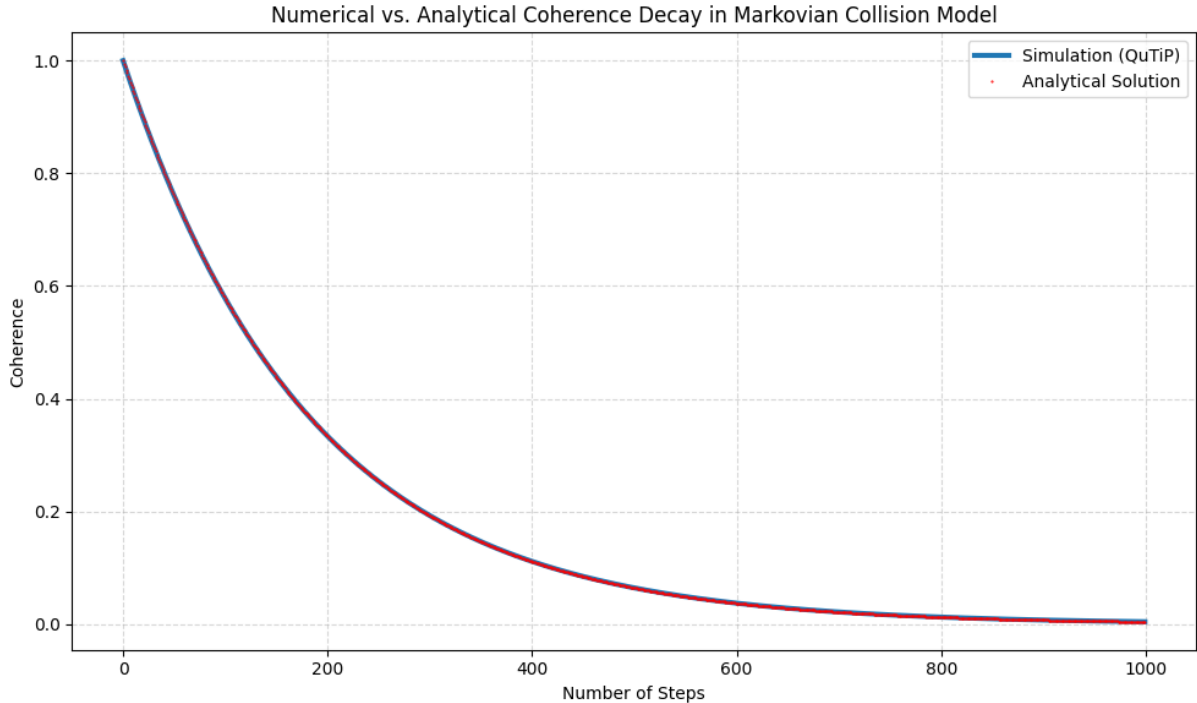


Figure 3.1 : Comparison of the analytical (solid line) and numerical (dots) results. The parameters are set to $g = 1$ and $\tau = \pi/30$.

3.1.2 Non-Markovian Strategy-1 Results

We now turn our attention to non-Markovian approaches. The first strategy involves introducing information loss at each unitary operation step. This is implemented via partial tracing of the density matrix. Physically, this operation corresponds to ignoring the degrees of freedom of the auxiliary particles (or environment) rather than performing a direct measurement. By tracing out the particles, we effectively degrade the entanglement within the multi-particle system, leading to a mixed state for the subsystem of interest.

This process results in the decoherence of the system. In a fully coupled, complete unitary evolution—as will be demonstrated in Strategy 2—the coherence is expected to oscillate reversibly. In contrast, the current approach exhibits damped oscillations, where the coherence decays over time due to the continuous information loss.

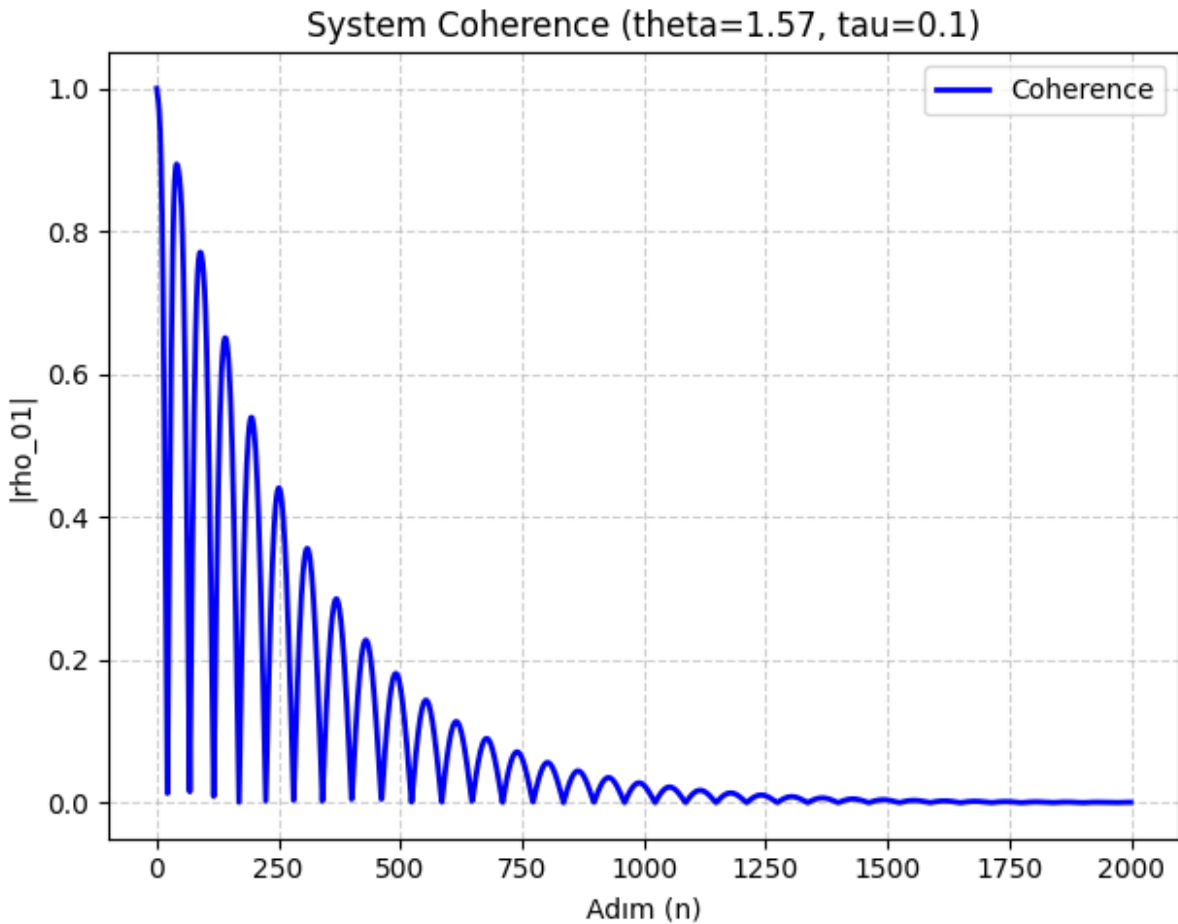


Figure 3.2 : Numerical solutions for strategy-1. The parameters are set to $g = 1$, system-ancilla $\tau = \pi/30$ and ancilla-ancilla $\theta = \pi/2$

The numerical results are further validated by comparing them with the analytical solution derived as $\cos^n(\tau)\cos(n\tau)$, where n denotes the number of steps and τ represents the small interaction parameter. As illustrated in Figure 3.4, the numerical simulation coincides perfectly with the analytical approach.

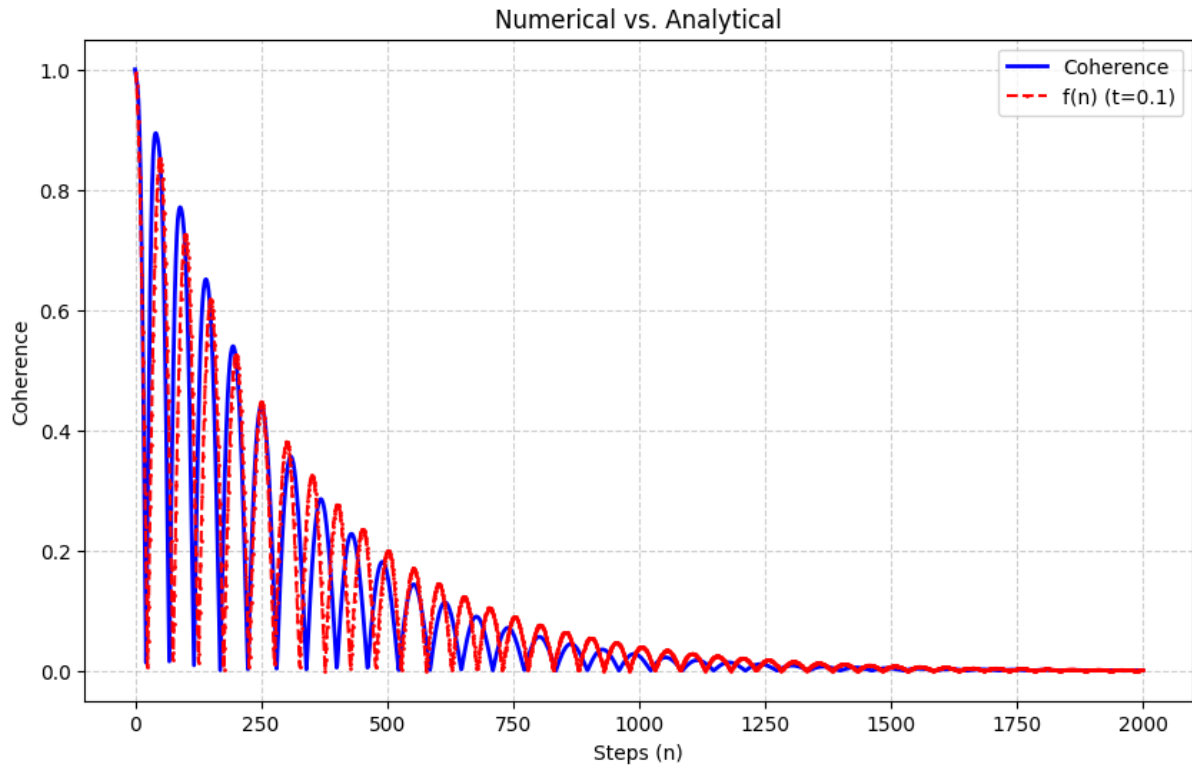


Figure 3.3 : Comparison of the numerical results with the analytical approach. The parameters are set to $g = 1$, system-ancilla $\tau = \pi/30$, and ancilla-ancilla $\theta = \pi/2$.

Furthermore, by introducing a slight detuning to the intra-environmental coupling parameter (setting $\theta = \pi/2.1$ instead of the resonant $\pi/2$), we observe a distinct oscillating decay pattern, resembling a "beating" phenomenon. Unlike the monotonic envelope observed in the resonant case, here the coherence exhibits amplitude modulation.

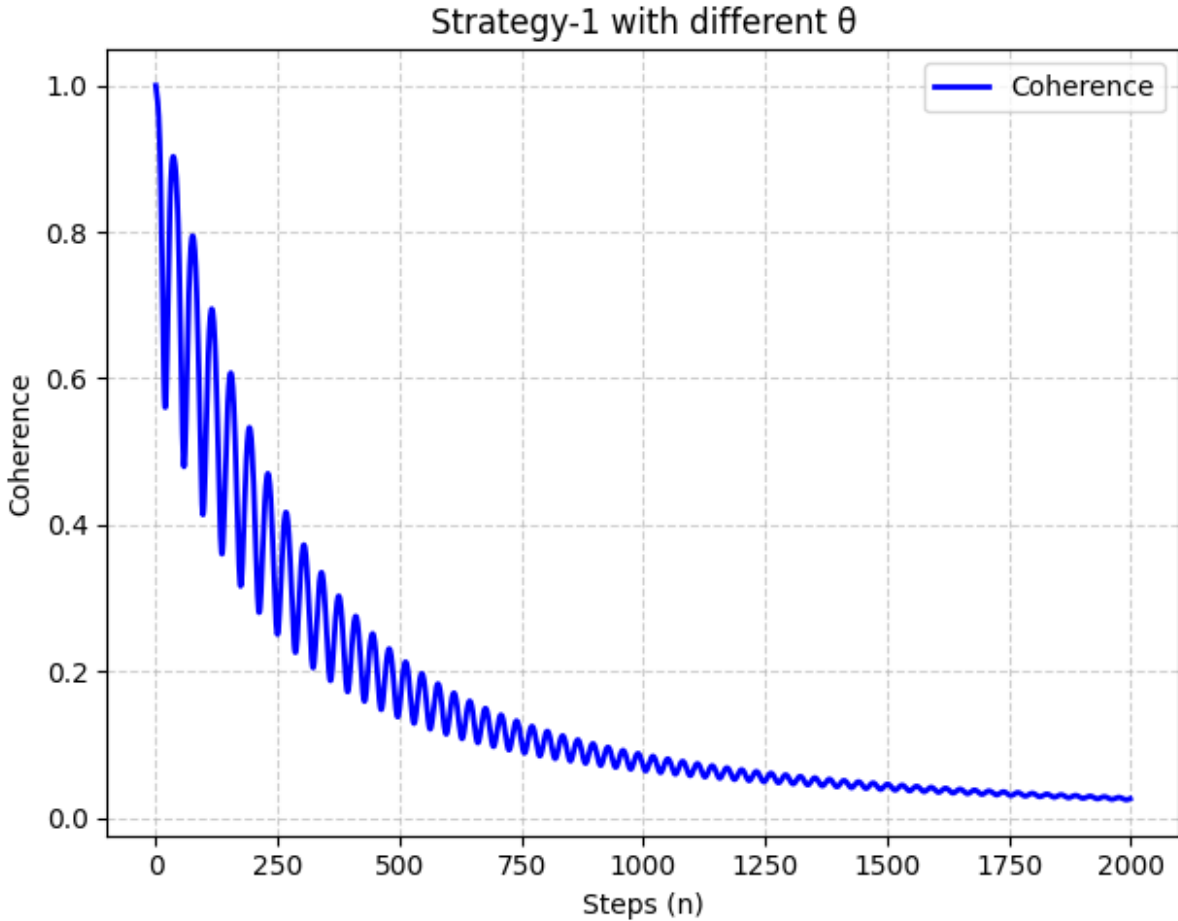


Figure 3.4 : The parameters are set to $g = 1$, system-ancilla $\tau = \pi/30$, and ancilla-ancilla $\theta = \pi/2.1$.

This behavior can be interpreted as the interference between the system-ancilla interaction frequency and the shifted ancilla-ancilla correlation frequency. While the overall trend remains a decay due to the iterative information loss (partial tracing), the detuning creates transient regimes where the decoherence rate is modulated, leading to the observed spring-like envelope.

3.1.3 Non-Markovian Strategy-2 Results

Having established the results for Strategy 1, we now introduce Strategy 2. In contrast to the previous approach, Strategy 2 involves delaying the partial trace operation. Specifically, the environment particle (ancilla) is traced out only *after* the ancilla-ancilla interaction has been fully completed.

This delay allows the correlation between the system, the current ancilla, and the outgoing ancilla to fully develop before any degrees of freedom are ignored. Since the interaction remains unitary and fully coupled within this window, there is no irreversible information loss. Consequently, the system exhibits reversible dynamics. As a result, the coherence does not decay monotonically; instead, it follows a sinusoidal pattern characterized by periodic cycles of **decoherence and revival**.

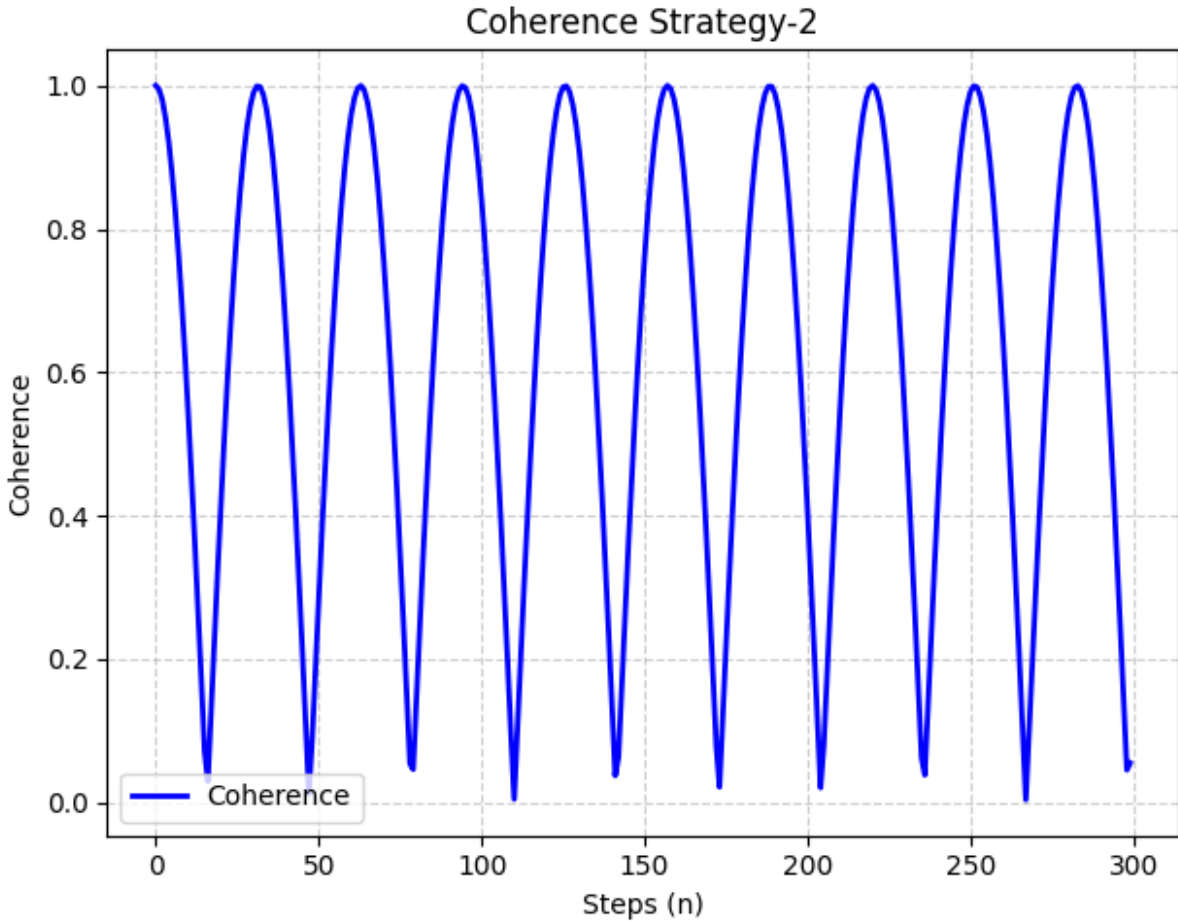


Figure 3.5 : Full decoherence and revival oscillations observed in Strategy 2. The parameters are set to $g = 1$, system-ancilla $\tau = \pi/30$, and ancilla-ancilla $\theta = \pi/2$.

However, a significant transition occurs when the ancilla-ancilla interaction parameter θ is detuned from the resonant $\pi/2$ value. In this regime, the interaction acts as a "partial SWAP" rather than a perfect information transfer. Consequently, the coherence no longer exhibits perfect revivals but starts to decay.

As illustrated in Figure 3.6, the decay profile features a distinct amplitude modulation (beating), strikingly similar to the behavior observed in the non-resonant regime of Strategy 1.

The physical origin of this decay differs from the Markovian case: here, the partial SWAP fails to transfer the complete correlation information to the incoming ancilla before the outgoing ancilla is traced out. This residual correlation remaining in the traced-out particle represents an irreversible information leakage from the system, leading to the observed damped oscillations.

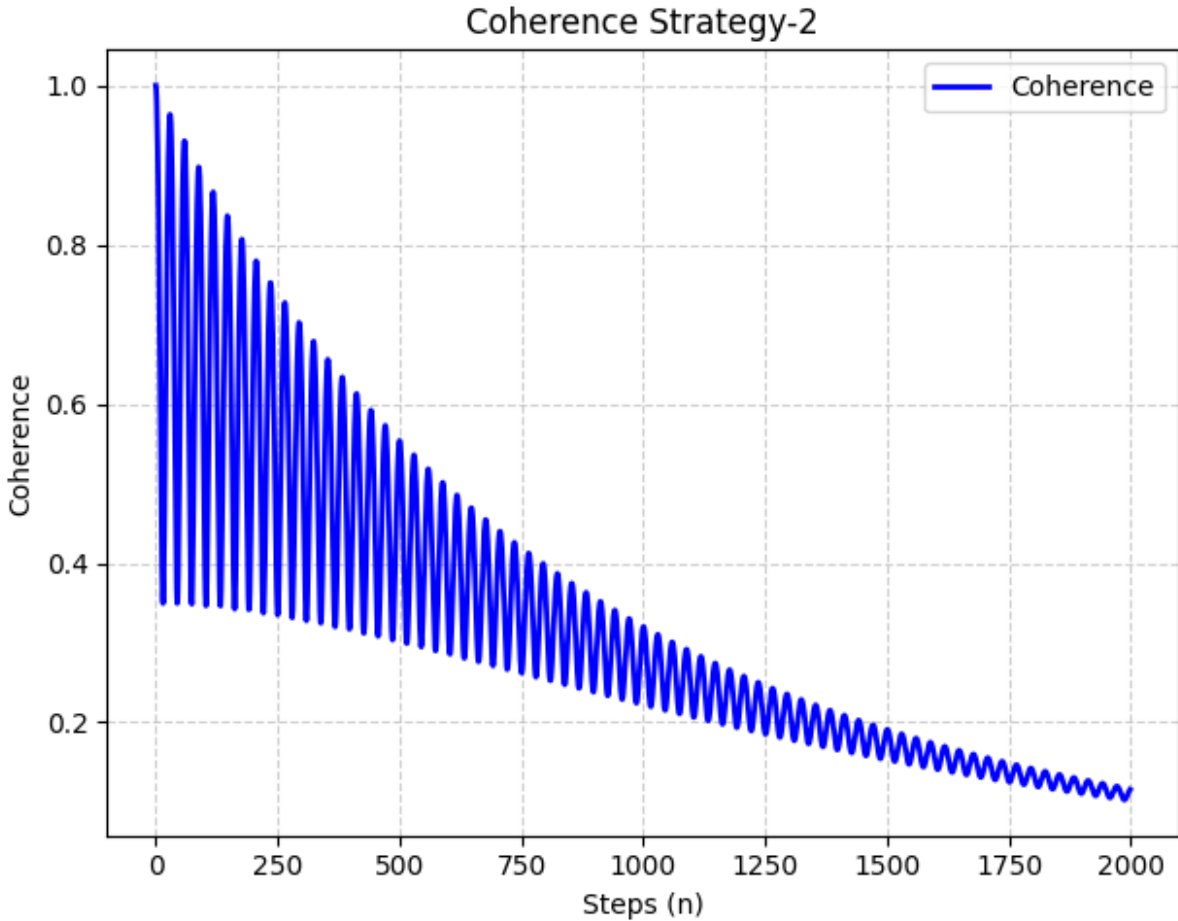


Figure 3.6 : Coherence evolution in Strategy 2 under partial SWAP conditions ($\theta \neq \pi/2$). The imperfect information transfer leads to information leakage during the trace-out step, resulting in a modulated decay.

3.2 Discussion

The results presented in this chapter demonstrate the versatility of collisional models in simulating both Markovian and non-Markovian quantum dynamics. A critical comparison between Strategy 1 and Strategy 2 reveals the fundamental role of *information backflow* in open quantum systems.

In the Markovian regime, the system loses information to the environment monotonically, as the bath correlation time is much shorter than the system's characteristic time scale. However, the non-Markovian approaches (Strategies 1 and 2) allow us to observe the effects of finite environmental memory.

The Role of Environmental Correlations

The most significant finding is the contrast between the damped oscillations of Strategy 1 and the full revivals of Strategy 2. In Strategy 1, although the system and ancilla interact, the immediate partial trace operation effectively resets the environment's state relative to the system, severing the build-up of long-term correlations. The observed "beating" pattern under detuning ($\theta \neq \pi/2$) indicates that even with information loss, the phase relationships between the system and the immediate ancilla create interference effects.

In contrast, Strategy 2 preserves the ancilla-ancilla correlations before the trace-out. This delay transforms the environment into a quantum memory. The full revivals observed at resonance ($\theta = \pi/2$) confirm that the information is not lost but temporarily stored in the collective state of the ancillas and then transferred back to the system. This corresponds to a regime of strong non-Markovianity where the information backflow is maximal.

Notably, our findings correlate well with the research conducted by McCloskey and Paternostro [7]. Although they employed trace distance (BLP measure) as the primary metric to quantify non-Markovianity, the dynamical behaviors observed in both Strategy 1 and Strategy 2 are qualitatively consistent with their results. This agreement suggests that, despite the difference in metrics, our collisional model successfully captures the essential regimes of information backflow and memory effects reported in the literature.

Decoherence as Information Leakage

The transition from perfect revivals to modulated decay in Strategy 2 (when θ is detuned) offers a clear physical interpretation of decoherence. When the intra-environmental interaction is not a perfect SWAP, the information transfer efficiency drops. The "leakage" of information occurs because the outgoing ancilla carries away residual correlations that were not successfully passed down the chain.

This suggests that controlling the internal dynamics of the environment (specifically the θ parameter) is as crucial as controlling the system-environment coupling strength (g or τ) for coherence preservation. These findings imply that such collisional models can serve as effective testbeds for developing reservoir engineering protocols, where the environment is structured specifically to protect the system's quantum state.

REFERENCES

- [1] **Zhao, M.J., Ma, T., Quan, Q., Fan, H. and Pereira, R.** (2019). l_1 -norm coherence of assistance, *Phys. Rev. A*, 100(6), <https://link.aps.org/doi/10.1103/PhysRevA.100.012315>.
- [2] **Zurek, W.H.** (1981). Pointer basis of quantum apparatus: Into what mixture does the wave packet collapse?, *Physical Review D*, 24(6), 1516–1525, <https://link.aps.org/doi/10.1103/PhysRevD.24.1516>.
- [3] **Zurek, W.H.** Environment-induced superselection rules, 26(8), 1862–1880, <https://link.aps.org/doi/10.1103/PhysRevD.26.1862>.
- [4] **Schlosshauer, M.** *Decoherence and the Quantum-To-Classical Transition*, Frontiers Collection, Springer Berlin Heidelberg, <http://link.springer.com/10.1007/978-3-540-35775-9>.
- [5] **Ciccarello, F., Lorenzo, S., Giovannetti, V. and Palma, G.M.** Quantum collision models: Open system dynamics from repeated interactions, 954, 1–70, <https://linkinghub.elsevier.com/retrieve/pii/S0370157322000035>.
- [6] **Şenyaşa, H.T., Kesgin, , Karpat, G. and Çakmak, B.** Entropy Production in Non-Markovian Collision Models: Information Backflow vs. System-Environment Correlations, 24(6), 824, <https://www.mdpi.com/1099-4300/24/6/824>.
- [7] **McCloskey, R. and Paternostro, M.** Non-Markovianity and system-environment correlations in a microscopic collision model, 89(5), 052120, <https://link.aps.org/doi/10.1103/PhysRevA.89.052120>.